Advanced Studies in Theoretical Physics
Vol. 18, 2024, no. 4, 203 - 221
HIKARI Ltd, www.m-hikari.com
https://doi.org/10.12988/astp.2024.92138

Stabilization Responses of an Infinite Porous Flow Channel Containing Ferrofluids

Azizah Alrashidi and Sameh A. Alkharashi *

Department of Laboratory Technology
College of Technological Studies, PAAET, Kuwait
* Corresponding author

Abstract

This paper investigates the effect of a magnetic field on the stability of two interfacial waves propagating between three infinite layers of viscous fluids. The flow propagates saturated in porous media so that liquids have distinct physical properties and are immiscible. The principal purpose of this study is to examine the impact of the porosity outcome and fluid viscosity on the growth rate in the existence of a magnetic field. In the horizontal axis direction. Fluid stability results from the amplitude of the waves and the extent to which they are affected by the interference between magnetic features and the effect of the media's porosity. The stability conditions are realized theoretically in which stability diagrams are achieved. The influence of the various quantities of the problem on the interface stability is thoroughly evaluated.

Keywords: Linear Stability; Normal Mode; Viscous Fluids; Magnetic Field; Porous Media

1 Introduction

The performance of moving films under certain circumstances has attracted many researchers due to their conceptual simplicity, rich dynamical

phenomenology, and technological relevance and has fascinated considerable interest since the pioneering experimental and theoretical reviews. The presentation of various pertinent studies that provide a useful summary of hydrodynamic stability is provided below. In paper [1], the stability investigation of a two-layer system in the presence of a normal electric field was analyzed. According to the authors, the electric field plays a dual role in the stabilization process. The method proposed in [2] was restricted to studying the dynamics of an interface separating two liquids in a vertical channel. In one of the layers, coupled non-linear evolution relations for the interface form and flow rate are obtained.

In article [3], the linear stability investigation of pressure-driven flow under viscous heating effect via a channel is carried out. A modified coupled OrrSommerfeld equation was obtained with a linearized energy equation. It was mentioned that viscous heating has a destabilizing impact. In light of the linear stability theory, the effects of the density ratio, liquid viscosity and surface tension on the instability of the planar sheet are discussed in [4]. It is noted that the greater velocity difference across each interface has a destabilizing effect on the liquid sheet, but the extent of the increased can vary. DiCarlo [5] has theoretically investigated the stability of the standard multiphase flow equations. However, he has demonstrated experimentally that the instability is associated with saturation or pressure overshoot occurrences in 1-D infiltrations.

Awasthi [6] investigated the linear Rayleigh-Taylor instability of two viscous electrically conducting liquids. The viscous potential flow theory, which states that viscosity only contributes through normal stress balance is used. In terms of growth rate and wave number, a quadratic dispersion equation is obtained. Zakaria *et al.* [7] have analyzed the effect of an externally applied electric field on the stability of a thin fluid film over an inclined porous plane, using linear and non-linear stability analysis in the long wave limit. Wray *et al.* [8] have investigated the evolution and stability of a wetting viscous fluid layer flowing down the surface of a cylinder, and surrounded by a conductive gas.

Alkharashi and Alotaibi [9] have investigated the effect of periodic velocity on the stability of two interfacial waves propagating between three layers of immiscible incompressible fluids. The flow propagates saturated in porous media under the influence of an electric field. This paper uses the viscous potential theory to simplify the mathematical procedure, by which viscosity is accumulated on the separating surface rather than in the bulk of fluids. Recently, Alrashidi and Alkharashi [10] have examined the electrohydrodynamic instability of three porous-bounded liquid films with two interfaces in the presence of

stream periodicity and an electric horizontal field. It is considered that liquids have distinct physical characteristics and are immiscible. Applying the linear theory to the equations of motion and the associated boundary conditions led to two coupled Mathieu-type equations with complex periodic coefficients.

In this article, the considered system is composed of a viscous fluid layer of finite thickness embedded between two semi-infinite fluids. The system is influenced by horizontal magnetic field. The objective of the present work is to investigate the mechanisms of stability of three porous layers of fluids in the presence of horizontal magnetic field. The plan of this work is as follows:

The structure of this paper is as follows. The theoretical framework is clearly stated in the following section, and the basic equations of motion and related boundary conditions are surveyed. The third section deals with the stabilization of the problem, while the fourth section considers the derivation of the characteristic equation. Numerical applications for stability configuration are the subject of section five. The conclusion and main findings are discussed in the final section.

2 Theoretical framework

This article considers a two-dimensional system of an infinite horizontal viscous liquid sheet of vertical height $2d$ restricted between two semi-infinite superposed incompressible viscous fluids. The coordinates system is chosen as x-axis is parallel to the direction of the fluid sheet flow, and the y-axis is normal to the fluid sheet with its origin located at the middle plane of the fluid sheet as shown in Fig. 1. The top fluid occupies the region $y \in (d, \infty)$ the inner fluid is limited in the region demonstrated by $y \in (-d, d)$ while the range $y \in (-\infty, -d)$ characterizes the lower fluid. The system is considered to be influenced by the gravity force $\mathbf{g}(0,\ g)$ in the negative y-direction. The two interfaces between the fluids are assumed to be well defined and initially flat and form the interfaces $y = -d$ and $y = d$. The two interfaces are parallel and the flow in each phase is every where parallel to each other. The surface deflections are expressed by $y = \xi_1(x, t)$ at $y = -d$ and $y = \xi_2(x, t)$ at $y = d$, where $y = \pm\ d$ are the equilibrium positions of the two interfaces, i.e. the positions without disturbances, $\xi_l, (l = 1, 2)$ is the size of the disturbance at a point.

To better understand the dynamic stability of the current problem, the governing equations and their associated boundary conditions are placed in the non-dimensional form. Depending on the geometry of the shape, half the

thickness of the middle layer d can be chosen as the characteristic length.

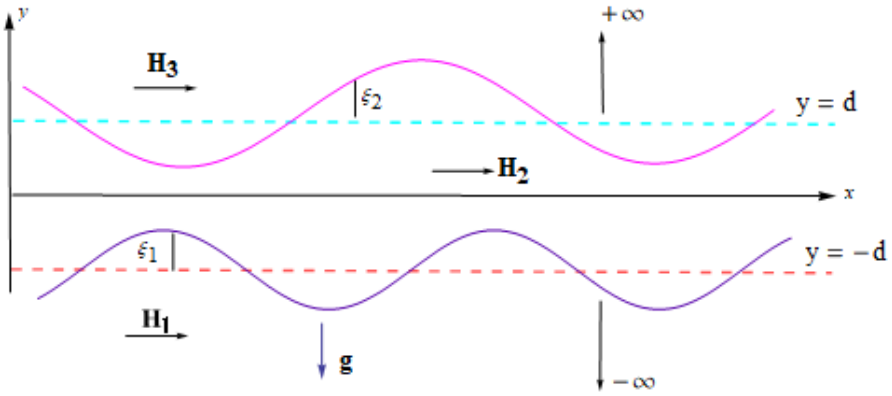

Figure 1: Sketch of problem geometry.

From the above, speed and time can be put in a dimensional form employing $\sqrt{dg}$ and $\sqrt{d/g}$. While the magnetic field and its potential take the non-dimensional form through $\sqrt{dg\rho_2/\mu_2}$ and $d\sqrt{dg\rho_2/\mu_2}$, respectively. In addition the pressure $dg\rho_2$, the stream function $\sqrt{d^3g}$, and the viscosity $\rho_2\sqrt{d^2g}$, as well as the permeability of the porous medium d^2Q.

Furthermore, in the equations of motion, we use the symbols: the fluid density ratio $\hat{\rho}_j = \rho_j/\rho_2$ $(j = 1, 2, 3)$ the dynamic viscosities ratio $\hat{\eta}_j = \eta_j/\eta_2$, and the magnetic permeability ratio $\hat{\mu}_j = \mu_j/\mu_2$. Also the Weber number $W_l = T_l/d^2g\rho_2$, $(\ l = 1, 2)$, where T_l is the surface tension coefficient.

2.1 *Governing equations*

Assuming a quiescent initial state, therefore the base state velocity in the fluid layers is zero in which the flow is steady and fully developed. Thus the fundamental nondimensional equations governing the motion of the magnetic fluids are coming out from the ordinary hydrodynamic equations and Maxwell's relations of magnetic field [8-12].

$$\hat{\rho}_j R_e\big\{\partial_t + (\mathbf{u}.\nabla)\big\}u_j = -R_e\partial_x\Pi_j + \hat{\eta}_j(\nabla^2 u_j + \frac{u_j}{Q_j}), \quad j = 1, 2, 3, \tag{1}$$

$$\hat{\rho}_j R_e\big\{\partial_t + (\mathbf{u}.\nabla)\big\}v_j = -R_e\partial_y\Pi_j + \hat{\eta}_j(\nabla^2 v_j + \frac{v_j}{Q_j}), \tag{2}$$

associated with the continuity equation which expresses the conservation of mass:

$$\partial_x u_j + \partial_y v_j = 0, \tag{3}$$

where $R_e = \rho_2\sqrt{d^3\mathrm{g}}/\eta_2$ denotes the Reynolds number of the middle layer and Q_j represents the permeability parameter and $\Pi_j = p_j + \rho_j gy$ stands for the

total hydrostatic pressure. In addition ∂_t is the partial derivative with respect to the time t, and $\nabla \equiv (\partial_x, \partial_y)$ is the horizontal gradient operator.

In formulating Maxwell's equations for the problem, we supposed that the electro-quasi-static approximation is valid for the problem, i.e. the effects of the magnetic fields due to the slow variations in the magnetic fields are negligible. This assumption requires the magnetic field to be both curl and divergence free and consequently we have

$$\nabla .\ (\mu_j\ \mathbf{E}_j) = 0, \tag{4}$$

$$\nabla \times \mathbf{E}_j = \mathbf{0}. \tag{5}$$

Here, $\mathbf{H}_j$ is the magnetic field intensity vector, the notation $\times$ refers to the vector product of two vectors and μ_j refers to the magnetic permeability. The construction of a potential function φ_j, can be representable as the gradient of the scalar potential such that

$$\mathbf{H}_j = (H_{0j} - \partial_x \varphi_j)\mathbf{e}_x - \partial_y \varphi_j \mathbf{e}_y, \tag{6}$$

automatically satisfies zero curl for a constant permittivity and therefore the electrostatic potential satisfies the Laplace equation

$$\partial_x^2 \varphi_j + \partial_y^2 \varphi_j = 0, \tag{7}$$

where $\mathbf{e}_x$ and $\mathbf{e}_y$ are unit vectors in $x-$ and $y-$ directions. It is to be noted here that the divergence of the Maxwell stress tensor in the bulk fluid is zero because the bulk of the fluid is free of net charge, and the magnetic permeability are independent of spatial position in the fluid. Thus, the Maxwell stress tensor not appear in the momentum equation above, but will affect the flow only through the conditions at the interface.

2.2 *Boundary conditions*

The boundary conditions that allow completing the solution of the above system of governing equations have to be specified. Since at the boundaries among fluids, the fluids and the magnetic stresses must be balanced. The components of these stresses consist of the hydrodynamics pressure, surface tension, porosity effects and magnetic stresses [13-16]. The boundary conditions represented here are prescribed at the interface $y = \xi_l(x, t)$, where ξ_l is the height of the disturbed interfaces away from its initial position ($y = \pm 1$) which is defined in the next section. As the interface is deformed all variables are slightly perturbed from their equilibrium values. Because the interfacial displacement is

small, the boundary conditions on perturbation interfacial variables need to be evaluated at the equilibrium position rather than at the interface. Therefore, it is necessary to express all the physical quantities involved in terms of Taylor series about $y = \pm 1$.

The flow field solutions of the above governing equations have to satisfy the kinematic and dynamic boundary conditions at the two interfaces, which can be taken as $y \approx \pm 1$ (the first order approximation for a small displacement of the interfaces due to the disturbance). The normal component of the velocity vector in each of the phases of the system is continuous at the dividing surface. This implies that

$$\mathbf{n}_l \cdot (\mathbf{u}_l - \mathbf{u}_{l+1}) = 0, \quad y = (-1)^l, \quad l = 1, 2, \tag{8}$$

where $\mathbf{n}_l$ is the outward normal unit vector to the interfaces which are given from the relation, $\mathbf{n}_l = \nabla S_l / \mid \nabla S_l \mid$ and $S_l(x, y, t)$ is the surface geometry defined by $S_l = y - \xi_l(x, t) = \pm 1$.
The condition that the interfaces are moving with the fluids ($D_t S_l = 0$) lead to

$$v_{l,(l+1)} + \partial_t \xi_l = 0, \quad y = (-1)^l, \quad l = 1, 2. \tag{9}$$

In addition the jump in the shearing stresses is zero across the interfaces, this gives

$$\left| \left[\hat{\eta}_l \ (\partial_y u_l + \partial_x v_l \right] \right|_l^{l+1} = 0, \quad y = (-1)^l, \quad l = 1, 2, \tag{10}$$

where, the notation $|[X]|$ is used here to signify the difference in some quantity X across the interfaces.

Furthermore, Maxwell's conditions on the magnetic field where no free surface charges are present on the interfaces. The continuity of the normal component of the magnetic displacement at the interfaces reads:

$$\mathbf{n}_l \cdot (\hat{\mu}_l \ \mathbf{H}_l - \mathbf{H}_{l+1}) = 0, \quad y = (-1)^l, \quad l = 1, 2, \tag{11}$$

which gives

$$\partial_y \varphi_2 - \hat{\mu}_1 \partial_y \varphi_1 = (\hat{\mu}_1 - 1) H_{01} \partial_x \xi_1, \quad y = -1,$$
$$\partial_y \varphi_2 - \hat{\mu}_3 \partial_y \varphi_3 = (\hat{\mu}_3 - 1) H_{01} \partial_x \xi_2, \quad y = 1.$$

The tangential component of the magnetic field is zero across the interfaces, this requires that

$$\mathbf{n}_l \times (\mathbf{H}_l - \mathbf{H}_{l+1}) = 0, \quad y = (-1)^l, \quad l = 1, 2, \tag{12}$$

from this equation, we have

$$\partial_x \varphi_2 - \partial_x \varphi_1 = 0 \quad \text{at} \quad y = -1 \quad \text{and} \quad \partial_x \varphi_3 - \partial_x \varphi_2 = 0 \quad \text{at} \quad y = 1.$$

The completion of the mathematical description of the problem requires an additional interfacial condition determine the shape of the interface between the fluids, which is the dynamical equilibrium boundary condition in which the surface traction suffers a discontinuity due to the surface tension:

$$\big|\big[\mathbf{n}_l.\ \tau\ .\mathbf{n}_l\big]\big|_l^{l+1} = W_l\ \nabla.\ \mathbf{n}_l, \qquad y = (-1)^l, \quad l = 1, 2. \tag{13}$$

The stress tensor, τ, is composed of a fluid component (isotropic pressure and deviatoric viscous stresses for the Newtonian fluid), $\tau^{(f)}$, and a magnetic component, $\tau^{(e)}$, whose expressions are given by the formulas

$$\tau_l^{(f)} = -p_l\mathbf{I} + \hat{\eta}_l(\nabla\mathbf{u}_l + \nabla\mathbf{u}_l^{T_r}), \tag{14}$$

$$\tau_l^{(e)} = \hat{\mu}_l\Big(\mathbf{H}_l\mathbf{H}_l - \frac{1}{2}\ \big(\mathbf{H}_l \cdot \mathbf{H}_l\big)\mathbf{I}\Big), \tag{15}$$

where the symbol $\mathbf{I}$ denotes the identity tensor, while the superscript T_r indicates the matrix transpose. Thus the dynamical condition becomes

$$\big|\big[\ -p + 2\hat{\eta}\frac{\partial v}{\partial y} + \hat{\mu}(E_n^2 - \frac{1}{2}E^2)\ \big]\big|_l^{l+1} = W_l\ \nabla \cdot \mathbf{n}_l. \tag{16}$$

3 Stabilization of the problem

In order to investigate the stabilization of the present problem, the interfaces between the fluids will be assumed to be perturbed about its equilibrium location and will cause a displacement of the material particles of the fluid system. This displacement may be described by the equation

$$\xi_l(x,t) = \hat{\xi}_l\ e^{ikx+\omega t} + c.c, \qquad l = 1, 2, \tag{17}$$

where $\hat{\xi}_l$ is the initial amplitude of the disturbance, which is taken to be much smaller than the half-thickness d of the middle sheet, k is the wave number of the disturbance, which is assumed to be real and positive ($k = 2\pi/\lambda$, where λ is the wavelength of the disturbance), ω is a complex frequency ($\omega = \omega_r + i\omega_i$, where ω_r represents the rate of growth of the disturbance, ω_i is 2π times the disturbance frequency), the symbol i denotes $\sqrt{-1}$, the imaginary number and $c.c$ represents the complex conjugate of the preceding terms.

The equations of motion and the boundary conditions mentioned previously will be solved under the assumption that the perturbations are small, so, all equations of motion and boundary conditions will be linearized in the perturbed quantities.

The solution of the above system of governing equations and boundary conditions can be facilitated by defining a stream function, ψ of the time and space coordinates, which automatically satisfies Eq. (3), where

$$u = \partial_y \psi, \ v = -\partial_x \psi. \tag{18}$$

Using the normal mode approach we write the perturbations in the form

$$\psi = \hat{\psi}(y) \ e^{ikx+\omega t} + c.c. \tag{19}$$

Eliminating the pressure term from Eqs. (1) and (2) and using (18) and (19), we obtain the following equation

$$D_y^4 \hat{\psi}_j - (\ell_j^2 + k^2) D_y^2 \hat{\psi}_j + k^2 \ell_j^2 \ \hat{\psi}_j = 0, \tag{20}$$

where $D_y = d/dy$ and

$$\ell_j = \Big\{ k^2 + \frac{\hat{\rho}_j \ R_e \ \omega}{\hat{\eta}_j} + \frac{1}{Q_j} \Big\}^{\frac{1}{2}}.$$

It is obvious that the analytical solution of Eq. (20) is of the form

$$\hat{\psi}_j(y) = A_{1j} \ e^{ky} + A_{2j} \ e^{-ky} + A_{3j} \ e^{\ell_j y} + A_{4j} \ e^{-\ell_j y}. \tag{21}$$

Since the boundary conditions require that the disturbances vanish as $y \to \pm\infty$ (i.e. $A_{21} = A_{41} = A_{13} = A_{33} = 0$). Thus we have the stream function in the three layers:

$$\begin{aligned}
\psi_1 &= (A_{11} \ e^{ky} + A_{31} \ e^{\ell_1 y}) \ e^{ikx+\omega t} + c.c, \quad y < -1, \\
\psi_2 &= (A_{12} \ e^{ky} + A_{22} \ e^{-ky} + A_{32} \ e^{\ell_2 y} + A_{42} \ e^{-\ell_2 y}) \ e^{ikx+\omega t} + c.c, \quad -1 < y < 1, \\
\psi_3 &= (A_{23} \ e^{-ky} + A_{43} \ e^{-\ell_3 y}) \ e^{ikx+\omega t} + c.c, \quad y > 1.
\end{aligned} \tag{22}$$

Using the normal mode solution we can obtain the pressure from Eqs. (1) and (2):

$$p_j = \frac{1}{ik} \Big\{ \frac{\hat{\eta}_j}{R_e} \ \Big[\partial_y^3 \psi_j + \partial_x^2 \partial_y \psi_j - Q_j^{-1} \partial_y \psi_j \Big] - \hat{\rho}_j \partial_x \partial_t \psi_j \Big\}. \tag{23}$$

The solution of the magnetic potential, in view of Eqs.(6) may be taken the form

$$\begin{aligned}
\varphi_1 &= B_{11} \ e^{ikx+ky+\omega t} + c.c, \quad y < -1, \\
\varphi_2 &= \big(B_{12} \ e^{ky} + B_{22} \ e^{-ky} \big) \ e^{ikx+\omega t} + c.c, \quad -1 < y < 1, \\
\varphi_3 &= B_{23} \ e^{ikx-ky+\omega t} + c.c, \quad y > 1.
\end{aligned} \tag{24}$$

4 Characteristic equation

In this section, we will derive the dispersion relation controlling the stability behavior of the system. When the obtained solutions of the stream function, magnetic potential and surface tension are inserted into Eqs. (8-16), we have a linear homogeneous system of algebraic equations of the fourteen unknown coefficients A_{pj}, B_{lj}, $\hat{\xi}_l$, $(p = 1, 2, 3, 4)$. This homogeneous system of equations can be expressed in matrix form as

$$\mathbf{AX} = \mathbf{0}, \tag{25}$$

where $\mathbf{0}$ is a null vector, $\mathbf{X}$ is a vector of unknown coefficients defined as

$$\mathbf{X}^{T_r} = \Big(\; A_{11}, \;\; A_{31}, \;\; A_{12}, \;\; A_{22}, \;\; A_{32}, \;\; A_{42}, \;\; A_{23}, \;\; A_{43},$$

$$B_{11}, \;\; B_{12}, \;\; B_{22}, \;\; B_{23}, \;\; \hat{\xi}_1, \;\; \hat{\xi}_2 \; \Big). \tag{26}$$

The coefficient matrix $\mathbf{A}$ is given in Appendix. A non-trivial solutions of the unknown coefficients A_{pj}, B_{lj}, $\hat{\xi}_l$, of the system (27) exists if and only if the determinant of the 14×14 matrix $\mathbf{A}$ must be equal to zero, which yields a dispersion relation between the wavenumber k and the perturbation frequency ω for specified values of other parameters, given by

$$F(\omega, k; R_e, H_{01}, \hat{\eta}_j, Q_j, W_l, \hat{\rho}_j, \hat{\mu}_j) = 0, \tag{27}$$

which represents the linear dispersion equation for surface waves propagating through a viscous layer embedded between two other fluids with the influence of constant horizontal magnetic field. This dispersion relation controls the stability in the present problem. That is, each negative of the real part of ω corresponds to a stable mode of the interfacial disturbance. On the other hand, if the real part of ω is positive, the disturbance will grow in time and the flow becomes unstable.

It is clear that the eigenvalue relation (28) is somewhat more general and quite complex, since ℓ_j involves square roots and so one can obtain other characteristic relation as limiting cases. For an inviscid fluid, we get the characteristic equation as a special case from Eq. (28) when $\eta_j = 0$. Thus by collecting the real and the imaginary terms in power order of ω with the help of symbolic computation software *Mathematica*, Eq. (28) can be transformed into a polynomial algebraic equation of fourth order in the frequency ω. Similar relations were obtained in the literature [13, 17] Also, in the special case when the effect of the magnetic forces is absent and for the fluids flow through

no-porous media, we get $\ell_j = \sqrt{k^2 + \frac{\hat{\rho}_j \ R_e \ \omega}{\hat{\eta}_j}}$ and in this case, the dispersion relation (28) is reduced to a non-polynomial algebraic equation for the frequency ω which coincides with that obtained by Kwak and Pozrikidis [18]. Another case is the limiting case of one interface between two continuum layers (non-porous medium), in which highly viscous fluids are considered. Thus we obtain a polynomial equation of fifth order in ω, which is obtained before by Kumar and Singh [14] and Sunil *et al.* [18].

In the following, numerical applications are carried out to demonstrate the effects of various physical parameters on the stability criteria of the system. In the present work, we will numerically solve the implicit dispersion relation by means of the Chebyshev spectral tau method [19].

5 Numerical applications

In order to discuss the stability diagrams, Eq. (28) is used to control the stability behavior, which requires specification of the parameters: the magnetic field, the magnetic permeability, the porosity effect, the density, the viscosity. In the calculations given below all the physical parameters are sought in the dimensionless form as defined above. The stability of fluid sheets corresponds to negative values of the disturbance growth rate (i.e. $\omega_r < 0$), and the disturbance growth rates of different fluids can be gained by solving the above corresponding dispersion relation numerically.

To screen the examinations of the magnetic field H_{01} and the magnetic permeability ratio $\hat{\mu}_3$ on the stability criteria, numerical calculations for the dispersion relation (28) are made. The results for calculations are displayed in Fig. 2 in the plane $(\omega_r - k)$. The graph displayed in this plane is evaluated for a system having the parameters given in the caption of Fig. 2. Before, we discuss the stability of this graph we firstly define the critical wave number (also called the cutoff wave number) as given in [22] the value of the wave number at the point where the growth rate curve crosses the wave number axis in the plots of wave growth rate versus wave number. In other words the critical wave number is the value of the wave number, which separates the stable motions from the unstable ones and conversely, and can be obtained from the corresponding dispersion relations by setting $\omega_r = 0$.

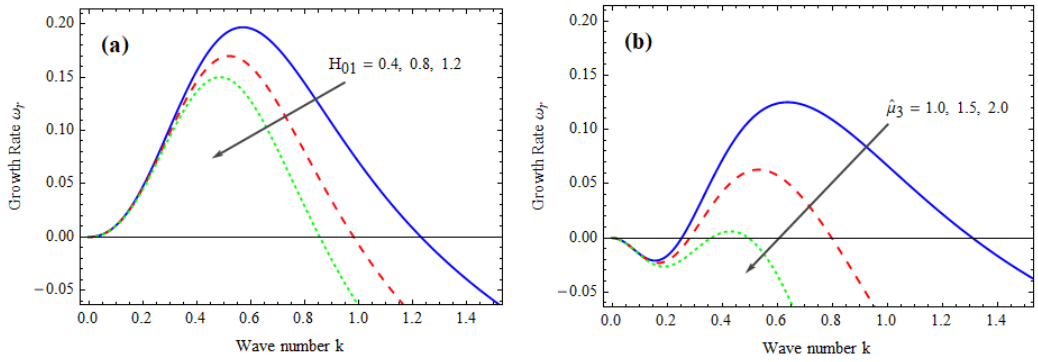

Figure 2: Effects of the magnetic field H_{01} and magnetic permeability $\hat{\mu}_3$ in the plane $(\omega_r - k)$ at $\hat{\mu}_1 = 1.2$, $\hat{\rho}_1 = 5$, $\hat{\rho}_3 = 2$, R_e=0.4, $\hat{\eta}_1$=0.2, $\hat{\eta}_3$=0.4, Q_1=0.1, Q_2 =0.2, $Q_3 = 0.3$, $W_1 = 2$, $W_2 = 1$ on the wave growth rate: part (a) at H_{01}=0.4 (solid), 0.8 (dashed), 1.2 (dotted) with $\hat{\mu}_3$=1.5, and part (b) at $\hat{\mu}_3$ =1.0 (solid), 1.5 (dashed),2.0 (dotted) with H_{01}=0.8.

In Fig. 2(a) the stability arises according to the negative sign of the real part of the complex frequency ω. Thus when the wave number is over the cutoff wave number, the fluid sheet is stable. In this figure the solid curve is plotted at the value $H_{01} = 0.5$, and the value $H_{01} = 1$ corresponds to the dashed line, while the dotted curve represents the value $H_{01} = 1.5$. The inspection of Fig. 2 part (a) indicates that as the magnetic field is increased both the growth rates and the cutoff wave numbers reduced, on other meaning the unstable regions under the curves are decreased. Therefore, it is concluded that the magnetic field effects has a stabilizing influence in the fluid sheets.

The influence of changes of the magnetic permeability ratio $\hat{\mu}_3$ $(= \mu_3/\mu_2)$, on the stability behavior in the plane $(\omega_r - k)$ is illustrated in Fig. 2(b). In the graph 2(b) the values 1.0, 1.5 and 2 are selected for $\hat{\mu}_3$ correspond to the continuous, dashed and dotted curves respectively. It is apparent from the inspection of Fig. 2(b), under the influence of the magnetic permeability $\hat{\mu}_3$, the growth rates with different magnetic permeability ratio keep almost identical for the wave numbers less than 0.25, but increase correspondingly at higher values of the wave number, further the plane $(\omega_r - k)$ is divided into two regions. The first is $0 < k < 0.25$, which represents a stabilizing effect for increasing the parameter $\hat{\mu}_3$. The second region lie in the range $0.25 < k < 1$, since in this range, we notice that, when the magnetic constant is increased, both the growth rates and the cutoff wave numbers of fluid sheets decrease. A general conclusion of the graph 3 reveals that the phenomenon of the dual (irregular) role is found for increasing the magnetic permeability ratio $\hat{\mu}_3$, which there are two roles one is a stabilizing influence in the range $k < 0.25$,

and the other is a destabilizing in the range $0.24 < k < 1.2$.

The examination of change of the lower to the middle fluid density ratio $\hat{\rho}_1$ in the stability criteria is illustrated in Fig. 3(a). The graphs are constructed for ω_r versus k, are achieved for three values of the ratio $\hat{\rho}_1$ =2, 4 and 6, correspond to the continuous, dashed and dotted lines respectively, where the other quantities are held fixed. In this figure, the areas lie under $k-$axis and above the curves are stable and may be called stability regions (corresponding to the negative values of ω_r), while the areas above the horizontal axis are unstable. The inspection of the stability diagram of Fig. 3(a) reveals that the increase of the density ratio $\hat{\rho}_1$ leads to increase in the width of unstable regions. The result that may be made here is that the ratio $\hat{\rho}_1$ has a destabilizing influence on the stability behavior of the waves. This result confirmed the fact that when the lower fluid is more heavier than the upper, thus the system is stable.

Fig. 3(b) exhibits the effects of the permeability parameter Q_1 on the stability behavior of the fluid layers.

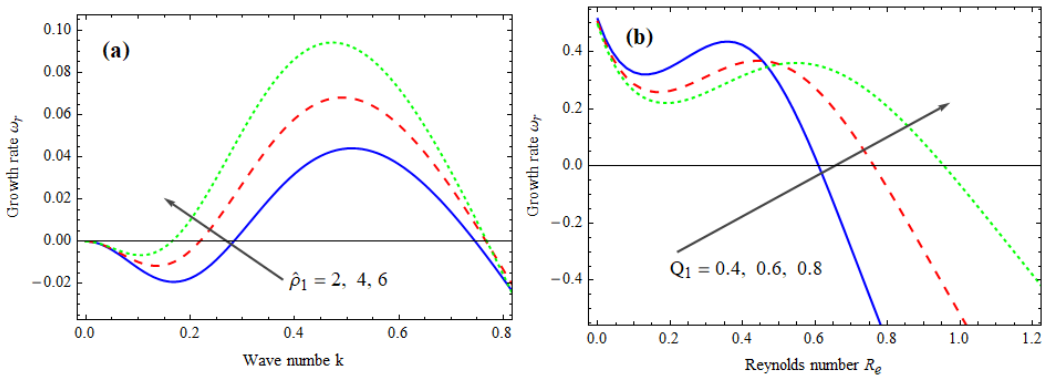

Figure 3: The graph is constructed for ω_r versus k, part (a) with $\hat{\rho}_1$=1, 2, 3 and against R_e part (b) with Q_1=0.4, 0.6, 0.8.

In this graph the solid, dashed and dotted curves represent the values 0.4, 0.6 and 0.8 in the plane $(\omega_r - R_e)$ of the parameter Q_1 respectively. Having noted the stability chart of this diagram, it is observed that the increase of the permeability in the range $0 < R_e < 0.5$, leads to a contraction in the width of the instability regions (the regions under the curves and above the wave number axis correspond to the positive sign of the disturbance growth rate). On the other hand, through the interval $0.5 < R_e < 1.2$ the growth rates of instabilities with different Q_1 are increased. In general view of the graph 3(b), it is noticed that there are two roles of the variation of the porous parameter Q_1, the first one is a stabilizing when the Reynolds number R_e less than the value 0.5, and the other role is a destabilizing when R_e lies between the values

0.5 and 1.2. Hence the phenomenon of the dual role is found for increasing the permeability parameter Q_1.

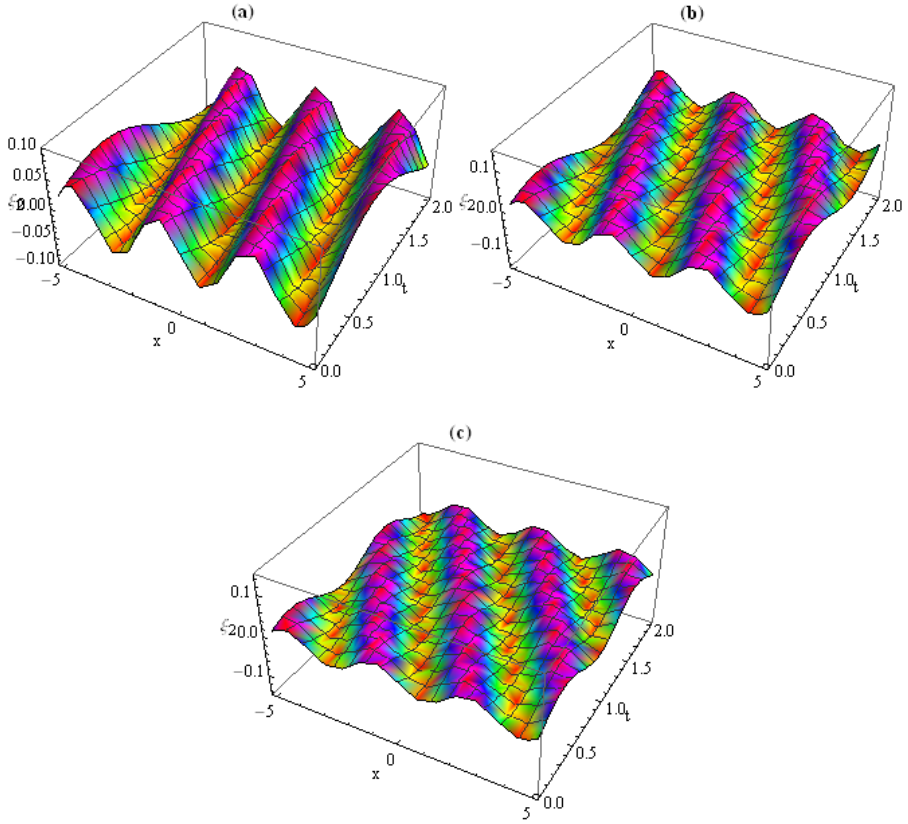

Figure 4: Three dimensions top interface elevation at $y = 1$, so that the viscosity ratio $\hat{\eta}_3$= 0.3, 0.5, and 0.7 are chosen for (a), (b), and (c), respectively.

Fig. 4 was produced in a three-dimensional system from the perspective of the height of the surface wave, where the horizontal direction of the waves' movement and the elevation of the upper interface were drawn versus time. The parts of this figure represent three different values of the viscosity ratio $\hat{\eta}_3$ for comparison while preserving the values of other variables as mentioned in the previous figure. A general inspection of this figure demonstrates that increasing the viscosity ratio $\hat{\eta}_3$ to a value of 0.5 in Fig. 4(b) leads to a contraction of the crests and troughs of the waves. However, another increase in $\hat{\eta}_3$ to become 0.7 in the third part of this graph leads to more contraction and shorter height of the crests and troughs. Hence, we conclude that the viscosity ratio of the top interface has a stabilizing effect on the shape of the interfacial wave elevation. From a physical point of view, we can justify the system's stability or not, that the greater the surface viscosity of the lower layer matched its higher counterpart. This leads to damping in the frequency

of the waves accordingly helping stabilize the fluid. In the opposite case, i.e., the surface viscosity in the upper layer is greater than the lower one, we get an unstable system.

Through images of instantaneous streamlines of the stream function [23-26], the impact Reynolds number is beginning to be realized in various portions of Fig. 5. All physical amounts are fixed to draw the streamlines contour, with the exception of the Reynolds number, which has three values (0.4, 0.6, and 0.8) that correspond to the parts (a)-(c).

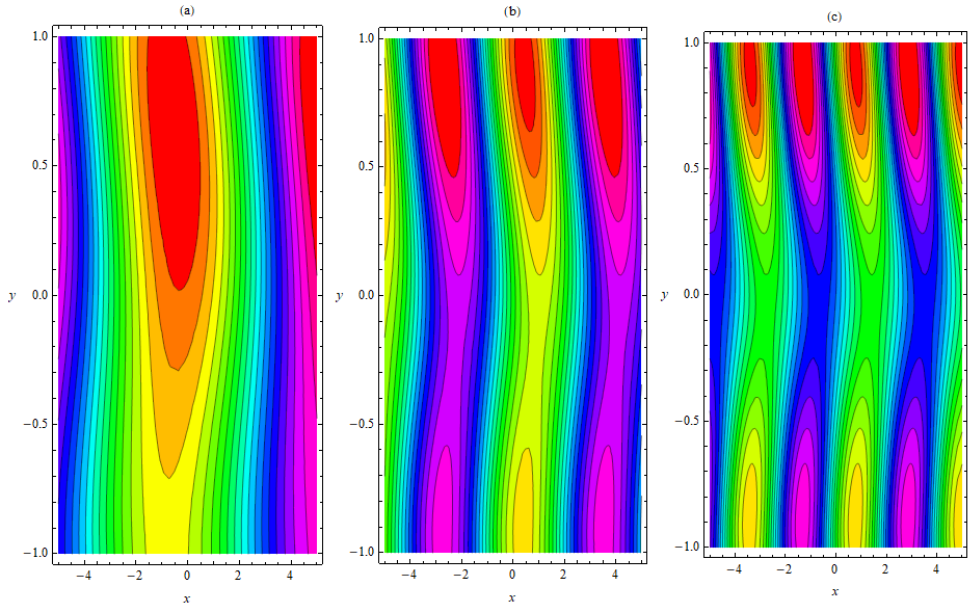

Figure 5: Streamlines contours for a system having the same parameters considered in Fig. 2, with $k = 0.5$, $t = 0.2$, $\hat{\xi}_1 = 0.02$ and $\hat{\xi}_2 = 0.06$, where $R_e = 0.5$, 1 and 1.5 of the parts (a), (b), (c) and (d), respectively.

An examination of the individual components of this figure reveals that the streamlined contours shift and speed up to (more than two cells) in the direction of the wave movement, as the Reynolds number increases. A conclusion that can be drawn from the similarity of the portraits (a-c) in Fig. 5, is that the destabilizing effect was caused by the crowding of the streamlines in the fluid movement's trend due to the enlarging Reynolds number. This behavior is consistent with the findings reported in the literature [27-29].

6 Conclusions

The current analysis considers the influence of a magnetic field on the stability of two interfacial waves propagating between three infinite layers of viscous

fluids. The flow propagates saturated in porous media so that liquids have distinct physical properties and are immiscible. Fluid stability results from the amplitude of the waves and the extent to which they are marked by the interference between magnetic features and the consequence of the media's porosity. The dispersion equation is obtained by solving the linear equations with the boundary constraints governing the problem under study. The dispersion formula depends on the growth rate and the wavelength and is an implicit relationship.

The stability of the fluid layers was examined analytically and numerically, by drawing some diagrams in which the physical scales are set in the dimensionless formula. Several outcomes can be drawn as realized based on the numerical survey, subject to certain constraints.

It is shown that the lower to the inner fluid density ratio develops both the growth rate and the instability range of the liquid sheet, which has a destabilizing effect. This result leads to the fact that when the upper fluid is lighter than the lower liquid, the system is in a stable state.

The dual role of both the porosity of the medium and the permeability of the magnetic field was observed. As a result of absorbing part of the kinetic energy, the viscosity coefficient and the magnetic field work to dampen the motion and thus lead to the stability of the system. Finally, both the Reynolds number and the density ratio work to expand the amplitude of the disturbance, which stimulates the instability of the liquid layers.

Appendix

The values of the coefficients of matrix A appearing in Eq. (25) are

$$\begin{pmatrix}
ike^{-k} & ike^{-\ell_1} & 0 & 0 & 0 & 0 & 0 \\
0 & 0 & ike^{-k} & ike^{k} & ike^{-\ell_2} & ike^{\ell_2} & 0 \\
0 & 0 & ike^{k} & ike^{-k} & ike^{\ell_2} & ike^{-\ell_2} & 0 \\
0 & 0 & 0 & 0 & 0 & 0 & ike^{-k} \\
2\hat{\eta}_1 k^2 e^{-k} & \hat{\eta}_1(k^2+\ell_1^2)e^{-\ell_1} & -2k^2e^{-k} & -2k^2e^{k} & -(k^2+\ell_2^2)e^{-\ell_2} & -(k^2+\ell_2^2)e^{\ell_2} & 0 \\
0 & 0 & 2k^2e^{k} & 2k^2e^{-k} & (k^2+\ell_2^2)e^{\ell_2} & (k^2+\ell_2^2)e^{-\ell_2} & -2\hat{\eta}_3 k^2 e^{-k} \\
ke^{-k} & \ell_1 e^{-\ell_1} & -ke^{-k} & ke^{k} & -\ell_2 e^{-\ell_2} & \ell_2 e^{\ell_2} & 0 \\
0 & 0 & ke^{k} & -ke^{-k} & \ell_2 e^{\ell_2} & -\ell_2 e^{-\ell_2} & ke^{-k} \\
0 & 0 & 0 & 0 & 0 & 0 & 0 \\
0 & 0 & 0 & 0 & 0 & 0 & 0 \\
0 & 0 & 0 & 0 & 0 & 0 & 0 \\
0 & 0 & 0 & 0 & 0 & 0 & 0 \\
\hat{A}_{11} & 2ik\ell_1\hat{\eta}_1 e^{-\ell_1} & \hat{A}_{12} & \hat{A}_{22} & -2ik\ell_2 e^{-\ell_2} & 2ik\ell_2 e^{\ell_2} & 0 \\
0 & 0 & \check{A}_{12} & \check{A}_{22} & 2ik\ell_2 e^{\ell_2} & -2ik\ell_2 e^{-\ell_2} & \check{A}_{23}
\end{pmatrix}$$

$$\begin{pmatrix}
0 & 0 & 0 & 0 & 0 & \omega & 0 \\
0 & 0 & 0 & 0 & 0 & \omega & 0 \\
0 & 0 & 0 & 0 & 0 & 0 & \omega \\
ike^{-\ell_3} & 0 & 0 & 0 & 0 & 0 & \omega \\
0 & 0 & 0 & 0 & 0 & 0 & 0 \\
-\hat{\eta}_3(k^2+\ell_3^2)e^{-\ell_3} & 0 & 0 & 0 & 0 & 0 & 0 \\
0 & 0 & 0 & 0 & 0 & 0 & 0 \\
-\ell_3 e^{-\ell_3} & 0 & 0 & 0 & 0 & 0 & 0 \\
0 & k\hat{\mu}_1 e^{-k} & -ke^{-k} & ke^{k} & 0 & ik(\hat{\mu}_1-1)H_{01} & 0 \\
0 & 0 & ke^{k} & -ke^{-k} & k\hat{\mu}_3 e^{-k} & 0 & ik(\hat{\mu}_3-1)H_{01} \\
0 & -ike^{-k} & ike^{-k} & ike^{k} & 0 & 0 & 0 \\
0 & 0 & -ike^{k} & -ike^{-k} & ike^{-k} & 0 & 0 \\
0 & -ik\hat{\mu}_1 H_{01}e^{-k} & ikH_{01}e^{-k} & ikH_{01}e^{k} & 0 & \check{\xi}_1 & 0 \\
2ik\ell_3\hat{\eta}_3 e^{-\ell_3} & 0 & -ikH_{01}e^{k} & -ikH_{01}e^{-k} & ik\hat{\mu}_3 H_{01}e^{-k} & 0 & \check{\xi}_2
\end{pmatrix} \tag{28}$$

where

$$\hat{A}_{11} = Q_1^{-1}e^{-k}\{Q_1(2i\hat{\eta}_1k^2 - \hat{\rho}_1\omega) - 1\},$$

$$\hat{A}_{l2} = Q_2^{-1}e^{(-1)^l k}\{\ Q_2(\omega + 2(-1)^l ik^2) + 1\}, \quad l = 1, 2,$$

$$\check{A}_{12} = e^{-k}(2ik^2 - \omega - Q_2^{-1}), \quad \check{A}_{22} = -Q_2^{-1}e^{-k}\{Q_2(\omega + 2ik^2) + 1\},$$

$$\check{A}_{23} = -Q_3^{-1}e^{-k}\{Q_3(2i\hat{\eta}_3k^2 + \hat{\rho}_3\omega) + 1\}, \quad \check{\xi}_1 = 1 - \hat{\rho}_1 + k^2W_1,$$

$$\check{\xi}_2 = -1 + \hat{\rho}_3 + k^2W_2.$$

Conflicts of Interest. The authors declare no conflict of interest.

Acknowledgements. This work was supported and funded by The Research Program of Public Authority for Applied Education and Training in Kuwait, Project No. (TS-23-05).

References

[1] F. Li, O. Ozen and N. Aubry, Linear stability of a two-fluid interface for electrohydrodynamic mixing in a channel, *J. Fluid Mech.*, **583** (2007), 347-377. https://doi.org/10.1017/s0022112007006222

[2] G.M. Sisoev, O.K. Matar, D. Sileri and C.J. Lawrence, Wave regimes in two-layer microchannel flow, *Chemical Eng. Science*, **64** (2009), 3094-3102. https://doi.org/10.1016/j.ces.2009.03.044

[3] K.C. Sahu and O.K. Matar, Stability of plane channel flow with viscous heating, *ASME J. Fluids Eng.*, **132** (1) (2010), 011202. https://doi.org/10.1115/1.4000847

[4] L.-J. Yang, B.-R. Xu, and Q.-F Fu, Linear instability analysis of planar non-Newtonian liquid sheets in two gas streams of unequal velocities, *J. Non-Newton. Fluid Mech.*, **167-168**, (2012), 50-58. https://doi.org/10.1016/j.jnnfm.2011.10.003

[5] D.A. DiCarlo, Stability of gravity-driven multiphase flow in porous media: 40 Years of advances, *Water Resour. Res.*, **49** (2013), 4522-4531. https://doi.org/10.1002/wrcr.20359

[6] M.K. Awasthi, Viscous potential flow analysis of magnetohydrodynamic RayleighTaylor instability with heat and mass transfer, *Int. J. Dyn. Control*, **2** (3) (2013), 254-261. https://doi.org/10.1007/s40435-013-0050-9

[7] K. Zakaria, M. A. Sirwah, S. A. Alkharashi, Non-linear analysis of creeping flow on the inclined permeable substrate plane subjected to an electric field, *Int. J. of Non-Linear Mech.*, **47** (2012), 577-598. https://doi.org/10.1016/j.ijnonlinmec.2011.11.010

[8] A.W. Wray, D.T. Papageorgiou and O.K. Matar, Electrified coating flows on vertical fibres: enhancement or suppression of interfacial dynamics, *J. Fluid Mech.*, **735** (2013), 427-456. https://doi.org/10.1017/jfm.2013.505

[9] S.A. Alkharashi, and W. Alotaibi, Structural stability of a porous channel of electrical flow affected by periodic velocities, *J. Eng. Math.*, **141** (3) (2023). https://doi.org/10.1007/s10665-023-10278-3

[10] A. Alrashidi, and S.A. Alkharashi, Modeling the Link Between Electric Fields and Three Films of Porous Channel Flow, *Journal of Engineering Science and Technology Review*, **17** (3) (2024), 1-7. https://doi.org/10.25103/jestr.173.01

[11] A. Samanta, Nonmodal stability analysis of Poiseuille flow through a porous medium, Advances in Water Resources 192 (2024) 104783. https://doi.org/10.1016/j.advwatres.2024.104783

[12] A. Katsiavria and D. T. Papageorgiou, Stability analysis of viscous multilayer shear flows with interfacial slip, *IMA Journal of Applied Mathematics*, **89** (2024), 279-317. https://doi.org/10.1093/imamat/hxae012

[13] S.A. Alkharashi, Khaled Al-Hamad and Azizah Alrashidi, On the Dynamic Regulation of Three-Layer Stratified Flow through Porous Media, *Advanced Studies in Theoretical Physics*, **12** (4) (2018), 197-217. https://doi.org/10.12988/astp.2018.8521

[14] N.M Hafez and A. Assaf, Electrohydrodynamic stability and heat and mass transfer of a dielectric fluid flowing over an inclined plane through porous medium with external shear stress, *Eur. Phys. J. Plus*, **138** (2023), 28. https://doi.org/10.1140/epjp/s13360-022-03615-5

[15] A. Assaf and S.A. Alkharashi, Hydromagnetic instability of a thin viscoelastic layer on a moving column, *Physica Scripta*, **94** (2019), 045201, 19p. https://doi.org/10.1088/1402-4896/aaf948

[16] S.A. Alkharashi, Kh. Al-Hamad and A. Alrashidi, Outlining the impact of structural properties of a multilayered porous channel with oscillating velocities and fields, *Dynamics of Atmospheres and Oceans*, (2023), 101366. https://doi.org/10.1016/j.dynatmoce.2023.101366

[17] K. Zakaria, M. Sirwah and .Alkharashi, Temporal Stability of Superposed Magnetic Fluids in Porous Media, *Physica Scripta*, **77** (2008) 1-20. https://doi.org/10.1088/0031-8949/77/02/025401

[18] S. Kwak, C. Pozrikidis, Effect of surfactants on the instability of a liquid thread of annular layer. Part I: Quiescent fluids, *Int. J. Multiphase Flow*, **27** (2001), 1-37. https://doi.org/10.1016/s0301-9322(00)00011-2

[19] P. Kumar and G.J. Singh, Stability of two superposed Rivlin-Ericksen viscoelastic fluids in the presence of suspended particles, *Rom. J. Phys.*, **51** (2006), 927-935.

[20] Sunil, R.C. Sharma and R.S. Chandel, On superposed couple-stress fluids in porous medium in hydromagnetics the Use of Quantum-Chemical Semiempirical Methods to Calculate the Lattice Energies of Organic Molecular Crystals. Part II: The Lattice Energies of - and -Oxalic Acid (COOH)2, *Z. Naturforsch. A*, **57a** (2002), 955-960. https://doi.org/10.1515/zna-2002-1208

[21] J.P. Boyd, *Chebyshev and Fourier Spectral Methods*, Dover Publications. Inc., Mineola, NY 2001. https://doi.org/10.1007/978-3-642-83876-7

[22] K. Zakaria, M. Sirwah and S. Alkharashi, Stability Behavior of Three non-Newtonian Magnetic Fluids in Porous Media, *Commun. Math. Sci.*, **9** (3) (2010), 767-796. https://doi.org/10.4310/CMS.2011.v9.n3.a6

[23] A. Haider, M.S. Anwar, Y. Nie and M.S. Alqarni, Exploring the role of nanoparticles in enhancing thermal performance of fractional Carreau fluid flow under magnetic field and hall current, *Case Studies in Thermal Engineering*, **59** (2024) 104537.
https://doi.org/10.1016/j.csite.2024.104537

[24] H.A. Hosham and N.M. Hafez, Global Dynamics and Bifurcation Analysis for the Peristaltic Transport Through Nonuniform Channels, *Journal of Computational and Nonlinear Dynamics*, **17** (2022), 061001-1.
https://doi.org/10.1115/1.4053668

[25] S. Goher, Z. Abbas and M.Y. Rafiq, Rheological properties of water-based Fe3O4 and Ag nanofluids between boundary layers due to shear flow over a still fluid, *Journal of Molecular Liquids*, **398** (2024), 124259.
https://doi.org/10.1016/j.molliq.2024.124259

[26] S.A. Alkharashi and Y. Gamiel, Stability Characteristics of Periodic Streaming Fluids in Porous Media, *Theoretical and Mathematical Physics*, **191** (1) (2017), 580-601.
https://doi.org/10.1134/s0040577917040092

[27] M. Ishaq, S. Ur Rehman, M. B. Riaz and M. Zahid, Hydrodynamical study of couple stress fluid flow in a linearly permeable rectangular channel subject to Darcy porous medium and no-slip boundary conditions, *Alexandria Engineering Journal*, **91** (2024), 50-69.
https://doi.org/10.1016/j.aej.2024.01.066

[28] S. A. Alkharashi and M.A. Sirwah, Dynamical Responses of Inclined Heated channel of MHD Dusty Fluids Through Porous Media, *J. Eng. Math.*, **130** (5) (2021). https://doi.org/10.1007/s10665-021-10160-0

[29] F.F. Dangharalou and M. Goharkhah, Effect of fluid properties on intensification of heat transfer process in oil-water droplet flow in a T-shaped microchannel, *Chemical Engineering & Processing: Process Intensification*, **200** (2024), 109799. https://doi.org/10.1016/j.cep.2024.109799

Received: October 15, 2024; Published: November 9, 2024